Journal of Materials Chemistry A

Accepted Manuscript

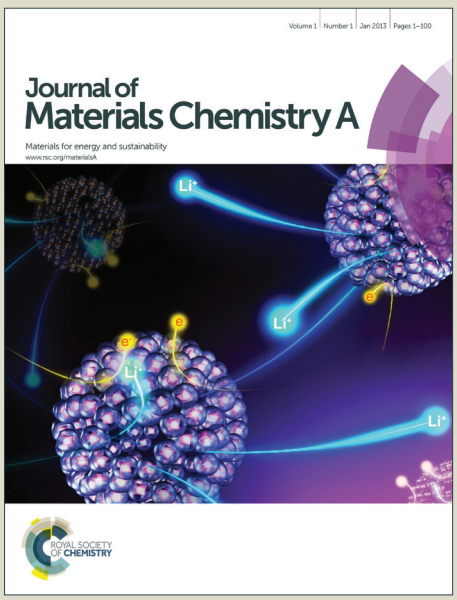

ROYAL SOCIETY OF CHEMISTRY

www.rsc.org/materialsA

Cite this: DOI: 10.1039/c0xx00000x

www.rsc.org/xxxxxx

ARTICLE TYPE

Highly efficient dye sensitized solar cells based on ordered and disordered mesoporous titania thick templated films

Reza Keshavarzi, Valiollah Mirkhani,* Majid Moghadam,* Shahram Tangestaninejad, Iraj Mohammadpoor-Baltork

Received (in XXX, XXX) Xth XXXXXXXXX 20XX, Accepted Xth XXXXXXXXX 20XX
DOI: 10.1039/b000000x

Ordered and disordered mesoporous titania thick films up to about 7 μm in thickness were successfully synthesized by an evaporation-induced self-assembly (EISA) process using dip and spin coating methods. To obtain crack-free thick films with high crystallinity and roughness factor we used a stabilization step after each coating and a calcination step after each five layers. Transmission electron microscopy (TEM), X-ray diffraction (XRD), scanning electron microscopy (SEM), BET analysis, ellipsometric analysis and UV-visible absorption spectroscopy (UV-vis) were used to characterize the microstructural features of the films. These mesoporous TiO_2 thick films were tested in dye-sensitized solar cells (DSSCs). The photovoltaic performances of cells made from meso-films prepared by dip and spin coating methods were compared and a maximum efficiency of 8.33% was achieved. This is the highest efficiency so far reported for DSSCs made from mesoporous titania templated films. The mesostructured films were compared with nanocrystalline TiO_2 films (NC-TiO_2) that are commonly used in DSSCs and showed superior performance.

Introduction

Dye-sensitized solar cells (DSSCs), first introduced by Grätzel and co-workers,[1] represent a promising alternative to photovoltaic cells because they can be fabricated using inexpensive materials and processes.[2]

Usually, DSSCs consists of a dye-adsorbed nanocrystalline TiO_2 layer with a thickness of 10-15 μm deposited on a transparent conductive oxide (TCO), electrolyte system and Pt counter electrode.[3–6]

Compared to nanocrystalline random porous TiO_2 films (NC-TiO_2), mesoporous TiO_2 templated film (meso-TiO_2) offers a large surface area, which allows more dye adsorption and hence, more efficient light absorption.

On the other hand, since all of the pores are regularly interconnected in mesoporous templated films, electrolyte diffusion will be highly efficient and meso-TiO_2 film will be a potential candidate for the photoanode in DSSCs.[7-11,46,47]

There are various approaches for synthesis of organized mesoporous films such as electrochemical techniques,[12-15] chemical solution deposition methods,[16-18] interface growth,[19-20] vapor phase impregnation,[22,23] and pulsed laser deposition.[24] Among these methods, the chemical solution deposition methods are the most employed. In this approach, the meso-ordering occurs through the evaporation induced self-assembly (EISA) mechanism.[25] Other approaches do not ensure good reproducibility and mesostractured control as well as EISA can.

The EISA is compatible with chemical solution deposition (CSD) techniques such as dip,[26,10] spin[27,45] and spray[28, 9] coatings. These techniques create a thin layer of mesoporous materials on the substrate. But the poor quantity of active material and, therefore, low surface area of these thin layers limit their practical applications. Therefore, to obtain better photovoltaic performances it is necessary to increase the film thickness by multilayer deposition.

First, Kavan and co-workers used ordered mesoporous TiO_2 photoanode in dye sensitized solar cells. The solar conversion efficiency of this mesoporous templated film bearing 1 μm thickness, prepared by EISA-dip coating technique, was about 50% higher than that of traditional films of the same thickness made from randomly co-oriented anatase nanocrystals.[30]

To more increase the efficiency of these cells, numerous activities and further investigation were carried out. Actually, mesoporous titania templated film is a semicrystalline network with the coexistence of anatase nanocrystals and a significant amount of amorphous titania. The low crystallinity always reduces the solar conversion efficiencies (< 1.25%).[31]

Prochazka *et al.* prepared the mesoporous thin layers and calcined them after each coating. This approach led to a high crystallinity with a decrease in the roughness factor.[32] While the thickness exhibits a constant increase, the roughness factor, related to the surface area, would not increase after 3–5 layers, and therefore, the photovoltaic performances reach a plateau.[32,33] Suitable phosphor-doping agents have been used for limiting the crystal growth. This led to preparation of 2.3 μm thick TiO_2 films with preserved roughness factor.[34] However, the solar conversion

efficiency of these films reached a plateau after eight layers. They attributed this observation to the charge collection, recombination and ohmic losses. Indeed, chemical doping should be avoided for DSSC application due to the possible modification of electronic structure, resulting in a higher probability of electron–hole recombination.[35,36] Alternatively, titania mesoporous thick temlated films were prepared by multilayer spin coating and a different thermal treatment route. In this method, a stabilization step was applied after each deposition cycle by heating the fresh film at moderate temperature on a hot plate during a few minutes. When the desired number of layers was deposited, the calcination step was done to overcome the surface area limitations induced by repeated calcinations.[37] Although many cycles were required to obtain a thick film by this method, but relatively good efficiencies were obtained. The disadvantage of this work was appearance of macro-cracks upon increasing the films thickness, which disturb the dye loading determination and promotes recombination inside the titania structure.[38] A dip-coating multilayer deposition following a similar heat treatment route was reported by Dewalque and co-workers. In this protocol, fewer layers need to obtain a thick film.[10] Despite the increasing dye loading and roughness factor (RF), a conversion efficiency plateau is reached after 9 layers due to the decrease of the open circuit voltage (Voc) values which is related to low crystallinity of films prepared by this method. The highest efficiency, obtained by the mesoporous titania photoanodes, is in the range of 6-7% for 5-6 µm films.[37] On the other hand, the cell performance is weakened when the film thickness is above ~3.5 µm, because of the serious film cracks.

All these attempts have been devoted to the improvement the microstructural features of films such as increasing their thickness while keeping a high porosity and crystallinity. But most of the reported procedures suffer from disadvantages such as time consuming procedures, up to one single layer per day,[30,32-34] too low thickness per layer,[37] and obvious limitation due to early arising of plateau in performances. Actually, some limitations such as low roughness factor, low crystallinity and formation of macro-cracks in the films lead to decrease of photovoltaic performance.

In this work, ordered and disordered mesoporous titania templated films with several micrometers in thickness were successfully synthesized via a layer-by-layer deposition. We used spin and dip coating techniques for preparation of mesoporous layers. The photovoltaic performances of the cells made by these two methods were compared and to decrease the limitations mentioned above, a new thermal treatment procedure was proposed. In this way to increase the RF, we used a stabilization step like Dewalque *et al.*[10] and Zhang *et al.*[37] but instead of one calcination step for mesoporous layers, the films calcined after each five layers.

This process not only increased the crystallinity, but also prevented the formation of cracks in the films.

To avoid the formation of cracks, the humidity ageing temperature and temperature of deposition were also changed from 25 °C to 20 °C. While most of the prepared mesoporous titania films for DSSCs have been aged (humidity aging) and deposited at 25 °C. This temperature causes cracks on the prepared films.[11,44] A 8.33% solar cell efficiency made of these mesoporous templated films was achieved. As far as we know, this is the highest efficiency obtained by the photoanodes made of the mesoporous TiO_2 templated films.

Experimental section

Mesoporous titania thick templated films synthesis

The mother solution was prepared according to the procedure reported by Zukalova *et al.*[30] In a typical procedure, concentrated HCl (Merck, 36% wt, 9.7 g,) was added to tetraethyl orthotitanate (Merck, 12.7 g) under vigorous stirring. Separately, block copolymer Pluronic P123 $[OH(CH_2CH_2O)_{20}(CH_2CH(CH_3)O)_{70}(CH_2CH_2O)_{20}H$, (Sigma-Aldrich, 4.0 g) was dissolved in 1-butanol (Aldrich, 36.3 g) and added to the $HCl/Ti(EtO)_4$ solution. This solution was aged by stirring at ambient temperature for at least 3 h. The films were prepared by dip coating (withdrawal rate of 0.8 mm/s) and spin coating (2000 rpm for 20 sec) of the solution onto substrates such as glass slides for the film mesostructure characterization or on FTO conducting glass (Dyesol, 15 Ω sq^{-1}) for the photovoltaic performance measurement. To obtain disordered mesoporous films, known as wormlike, by dip coating technique, the relative humidity (RH) in the electronic dip-coating chamber was set at 25–30%, and to obtain the mesoporous films with the same mesostructure by spin coating technique, the relative humidity in the electronic spin coating chamber was set at 45-50%. To obtain the ordered mesoporous films, known as gridlike, by dip coating technique, the relative humidity (RH) in the dip-coating chamber was set at 25–30% at 20 °C and the as-obtained films were directly transferred into an electronic ageing chamber under a controlled humidity of 75% during 24 h, and the layers prepared by spin coating were transferred into an electronic ageing chamber under a controlled humidity of 60% during two days. The deposition of several layers is possible by the intercalation of a stabilization step between each coating cycle. This stabilization is performed by heating the fresh film for 15 min on a hot plate pre-heated at 300 ºC. This leads to partial condensation of the inorganic network which prevents the redissolution of the film in the next dip or spin coating step. Solvent and water evaporation, as well as partial contraction and pore merging, also take place during the heat treatment.[10] After stabilizing of each five layers, the film was calcined under air at 350 ºC for 2 h (heating rate: 1 ºC/min) to prevent the formation of cracks in the film probably due to sudden heating and cooling the films in the stabilization step. For the preparation of thicker films, the described procedure was repeated. Finally, the film was calcined at 450 ºC for 1 h (heating rate: 1 ºC/min) to fully condense the inorganic network, increase the nanocrystallinity of the mesoporous TiO_2 films, crystallize the anatase phase and burn out all surfactant residues, leading to an anatase mesoporous structure.[10,37]All prepared thick samples were crack free and optically transparent.

Synthesis of Non-organized nanocrystalline titania thick films

For comparison, a standard non-organized nanocrystalline TiO_2 (NC-TiO_2) film was synthesized according to the method reported by Mallouk and coworkers.[39] In a typical procedure, tetraisopropyl orthotitanate (35.52 g) and anhydrous isopropanol (10 ml) were mixed well in a separatory funnel.

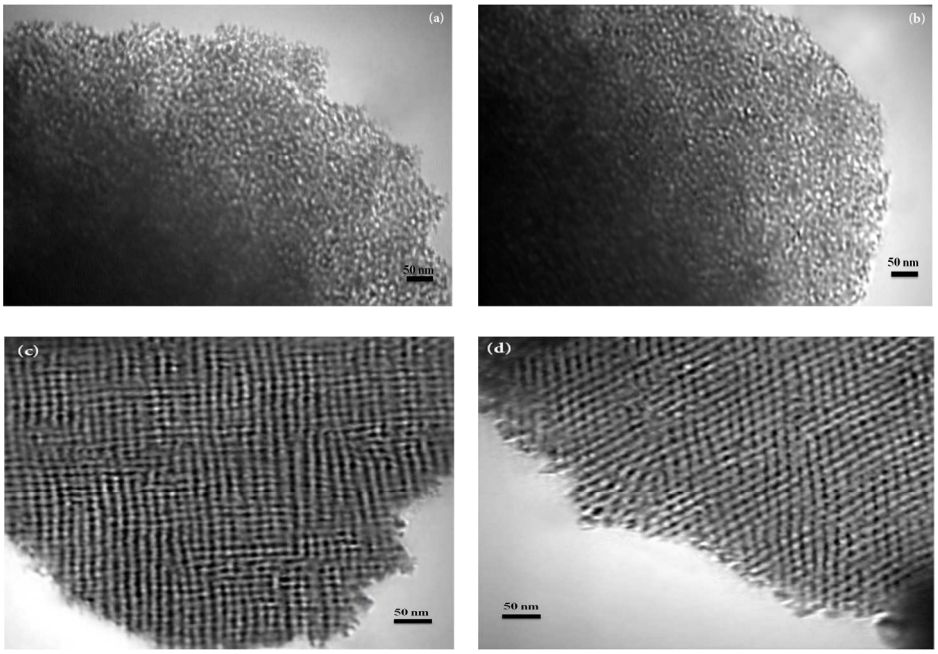

Figure 1. TEM images of the disordered wormlike mesoporous titania films prepared by: (a) dip and (b) spin coating. TEM images of the ordered gridlike mesoporous titania films prepared by: (c) dip and (d) spin coating techniques.

This solution was then added drop-wise to a prechilled solution (0 ºC in a dry ice/acetone bath) of acetic acid (80 mL) in deionized water (250 mL) in a round-bottom flask over a period of 20-30 min. During this time, the mixture was stirred rapidly by a magnetic stirring bar. The reaction solution was then heated to 80 ºC and stirred rapidly for 8 h. Then, the mixture was cooled down to the room temperature, sonicated for 5 min, autoclaved at 230 ºC for 12 h and then sonicated again for 5 min. The final concentration of TiO_2 was adjusted to 12 wt% with respect to total weight of solution. Hydroxypropylcellulose (HPC) was then added over 3-5 min to the rapidly stirred solution. The final HPC concentration was 6 wt% with respect to total weight of solution. The TiO_2 paste was first rapidly stirred for 24 h to dissolve HPC and the paste was continuously stirred with a lower speed until its use. Following this step, a few drops of prepared NC-TiO_2 paste was deposited and spread onto slides of glass or FTO by Doctor-Blade method. The prepared NC-TiO_2 thick layer was then calcined under air at 400 ºC for 8 h.

Fabrication of DSSCs

During the cooling process, the TiO_2 films coated on FTO substrates taken out of the furnace at 150 °C, then sensitized. The samples were slowly immersed into a 0.3 mM solution of N719 ruthenium dye (solaronix) in ethanol. All samples were sensitized for 48 h. The dye-adsorbed photoanode electrode was then rinsed thoroughly with ethanol and dried. After sensitization, the active area of the TiO_2 film was made to be 0.25 cm^2 by scraping away the excess. Counter electrodes were composed of a FTO conducting glass substrate (solaronix, 7 Ωsq^{-1}) coated by a platinum layer to catalyze electron transfer. This Pt coated FTO was prepared by dropping a 0.5 mM H_2PtCl_6 solution in anhydrous isopropanol on an FTO glass followed by heating at 385 °C for 15 min in air before cell assembly. The electrolyte consist of 0.6 M 1,2-dimethyl-3-propylimidazolium iodide, (98%, Ionic Liquids Technology), 0.05 M I_2, 0.1 M lithium iodine (LiI, Aldrich Chemical), and 0.5 M 4-*tert*-butylpyridine (TBP, Aldrich Chemical Company) and 0.1 M guanidium thiocyanate in acetonitrile (Aldrich Chemical Company). Stretched parafilm was used as a 20~30 µm spacer between the anode and platinum counter electrode. A drop of the redox electrolyte was placed on top of the active area and the platinized FTO glass counter electrode was placed on it and secured using binder clips.

Characterization techniques

The crystalline phase and crystallinity of titania present in the mesoporous films, was characterized using XRD technique with a Bruker D8 Advance X-ray diffractometer at room temperature, with monochromated Cu K_α (l = 1.54 Å) in a scan rate of 0.03 (2θ/s). The conditions of vacuum, accelerating voltage and the applied current were 5×10^{-5} mbar, 5.8 kV and 18 A, respectively. The rate of evaporation was controlled within the range 2.5-3 A°/s. A Phillips-CM200 transmission electron microscope (TEM) was used to investigate the morphology of the mesoporous films. The film texture and thickness were studied by a KYKY-EM3200 scanning electron microscope (SEM). For porosity measurements, the refractive indices of the mesoporous films were measured using an ellipsometer (SENTECH, SENpro). From these refractive indices, porosities were calculated using the Lorentz–Lorentz equation as follows:[40]

$$1\text{-}P = \frac{N_f^2-1}{N_f^2+2} \div \frac{N_a^2-1}{N_a^2+2} \quad (1)$$

It has to be mentioned that ellipsometric measurements can be

illusory for films thicker than 2 micrometer. Therefore, for films with a thickness higher than that, the thickness was checked by using cross-sectional SEM micrographs. Thermogravimetric measurements (TG/DTG) were performed by a thermal analysis instrument (Perkin Elmer, STA 6000). Sample was heated under air with a ramp of 2 ºC min^{-1}. Brunauer-Emmett-Teller (BET) measurements were carried out using a Belsorp-mini II system with N_2 as the adsorbate after the samples were carefully scratched off the substrate. The dye loading were recorded by a double-beam spectrophotometer (Cary 500 Scan Spectrophotometers, Varian). The amount of adsorbed dye was measured by the reported method.[10]

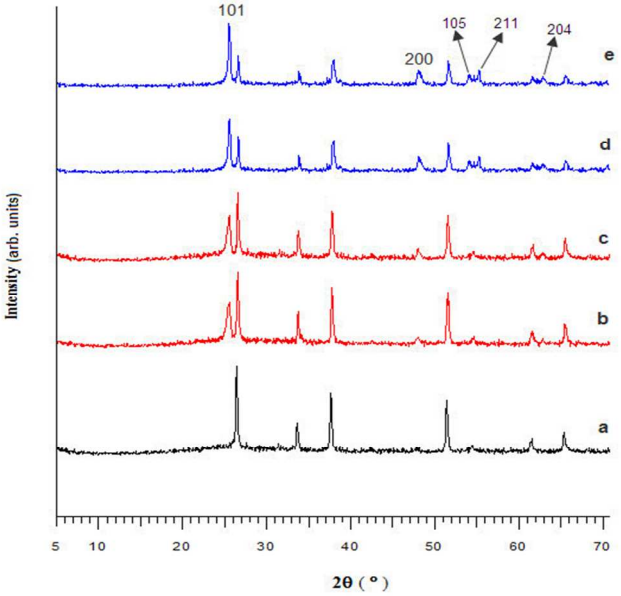

Figure 2. XRD patterns of: (a) FTO substrate, and (b) and (c) wormlike mesostructures related to 5.7 µm film prepared by dip and spin coating methods, respectively, (d) and (e) XRD pattern of the gridlike mesostructures related to 5.7 µm film prepared by dip and spin coating techniques, respectively. The unsigned diffraction peaks are related to the FTO substrate.

Photovoltaic performances of films have been evaluated by a solar simulator (Luzchem, v1.2) coupled with a µ-Autolab type III (Ecovchemie, Utrecht, the Netherlands) controlled by a microcomputer with Nova 1.7 software. Photocurrent-voltage measurements of the cell samples were performed under a simulated AM 1.5 solar illumination at an intensity of 100 $mWcm^{-2}$. A black mask with an aperture slightly larger (0.6 × 0.6 cm^2) than the active area of the solar cell (0.5 × 0.5 cm^2) was applied to avoid significant additional contribution from light falling on the device outside the active area. The incident photon to current conversion efficiency (IPCE) was carried out with spectral response measuring equipment (CEP-1500).

Results and discussion

Structural analysis of mesoporoustitania films

Ordered and disordered mesoporous titania films prepared by dip and spin coating techniques were analyzed by TEM. As shown by TEM images, the samples deposited under 25% RH and directly stabilized at 300 ºC present a disordered mesostructure known as wormlike (Fig. 1a and 1b). While, the films prepared by both dip and spin coating methods under 25% RH and ageing at high relative humidity before stabilization step present an ordered mesostructure known as gridlike. This is in accordance to other reports that suggest a higher relative humidity leads to more ordered mesostructure.[10,41-43] No crack was observed on the surface of the films due to the careful tuning of thermal treatments and also deposition and ageing at low temperature. The cracks may be caused by incomplete ordering of the inorganic matrix due to the fast hydrolysis and condensation, resulting in rapid film densification and pore collapse which is promoted by the relatively high temperature. Lower temperature aging allows the block copolymer micelles much more opportunity to self-assemble over longer length scales due to the slow hydrolysis and polycondensation reactions.[11,44]

Fig. 2 shows the XRD patterns of mesoporous TiO_2 films deposited on FTO coated glass substrates. The major peak at 2θ=25.4º corresponds to (101) reflection of the anatase phase, which is present in all prepared mesoporous TiO_2 films. The other peaks in XRD patterns are related to the (200), (105), (211), and (204) planes of the anatase phase, respectively. The crystallite size of anatase nanocrystals is calculated by the Scherrer equation. The crystallites size in the gridlike mesoporous films prepared by dip and spin coating methods were about 12.5 and 14 nm, respectively, and for the wormlike mesoporous films obtained by dip and spin coating methods were 10.5 and 11 nm, respectively.

As shown in Fig. 2d and 2e, the grid-like mesoporous films have a stronger (101) anatas peak than the wormlike mesostructure films (Fig. 2b and 2c). In other words, grid-like films are more crystalline than worm-like films. This may be due to higher RH which can result in more hydrolysis and polycondensation of inorganic species in the hybrid framework and thus generation of larger TiO_2 nanocrystallites after calcination.[11] On the other hand, the gridlike film prepared by spin coating method is more crystalline than the film prepared by dip coating method. It can also be related to more ageing time for ordered mesoporous films prepared by spin coating method.[11] The worm-like meso films prepared by spin coating method are a little more crystalline than the films prepared by dip coating method. This can be related to higher relative humidity in the spin coating chamber. However, it seems that ageing time play a more important role in the crystallinity of the films because of the much more crystallite size in the grid-like films compared to worm-like films. It is obvious that the number of calcination steps will increase the crystallinity.[31] Three and four calcination steps were carried out for obtaining the films bearing the thickness about 5.7 µm in the dip and spin coating methods, respectively. It can be another reason for higher crystallinity in mesoporous films prepared by spin coating method. However, it is clear that all of the wormlike and gridlike mesoporous titania films prepared by both dip and spin coating techniques have a high crystallinity.

As can be seen from TG and DTG thermograms of P123 pluronic surfactant in Fig. 3, thermal degradation starts from 205 ºC and total elimination of the surfactant is reached at around 330 ºC. It is expected that successive coating steps can lead to partial pores filling due to the introduction of inorganic precursor

solution into the porosity of the previous layer. This effect is likely to take place when the films are calcined between each step (i.e. 2 h at 350 ºC), leading to the elimination of the template and the opening of pores. Stabilization at 300 ºC should also lead to substantial elimination of the P123 copolymer. Thus, if there is no pore filling, the percentage of porosity should remain constant layer after layer.

Porosity percentage of films, obtained by ellipsometric analysis, is listed in the Table 1. The results clearly show no decrease in the porosity percentage of P123-templated mesoporous films with the number of layers. This can be related to pre-existing P123 micelles in the precursor solution.[32] During the stabilization step at 300 ˚C, the film undergoes a slight thermal contraction, therefore hindering the penetration of the micellar precursor solution into the opened pores during subsequent coating steps.[10] Actually, the close packing of the fused particles on the P123-originating pores makes the structure similar to the inversion opal.[32] The data in the Table 1 also show that the calcination at 350 ˚C after five layers and then coating of the sixth layer does not reduce the porosity percentage. Meanwhile, the wormlike mesostructure films had a more porosity than gridlike mesostructures. This might be a confirmation of the fact that the gridlike mesostructures had a larger crystallite size than wormlike mesostructures. As a result, the porosity percentage of the mesoporous films with a similar thickness prepared by our protocol decreases by increasing the crystallite size.

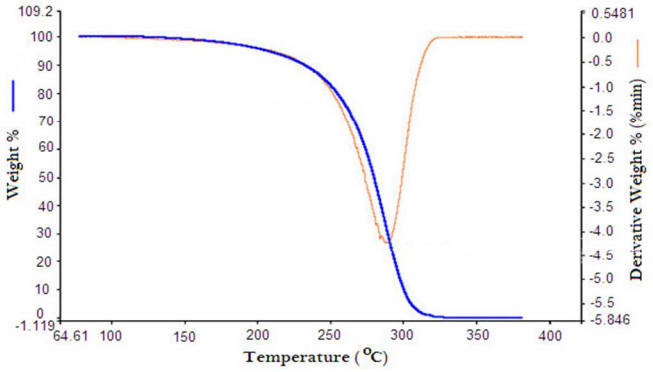

Figure 3. TG and DTG curves of P123 pluronic surfactant.

Table 1. Ellipsometric data for mesostructured thin films as a function of the number of layers.

Mesoporous Film	No. of layers	Thickness/nm	Porosity (%)
Wormlike-dip coating	1	405	43
	3	1168	42.5
	6	2275	42.5
Wormlike-spin coating	1	323	40
	3	920	40
	6	1799	39.5
Gridlike-dip coating	1	420	38
	3	1249	37.5
	6	2260	37.5
Gridlike-spin coating	1	350	36.5
	3	1020	36.5
	6	2075	36

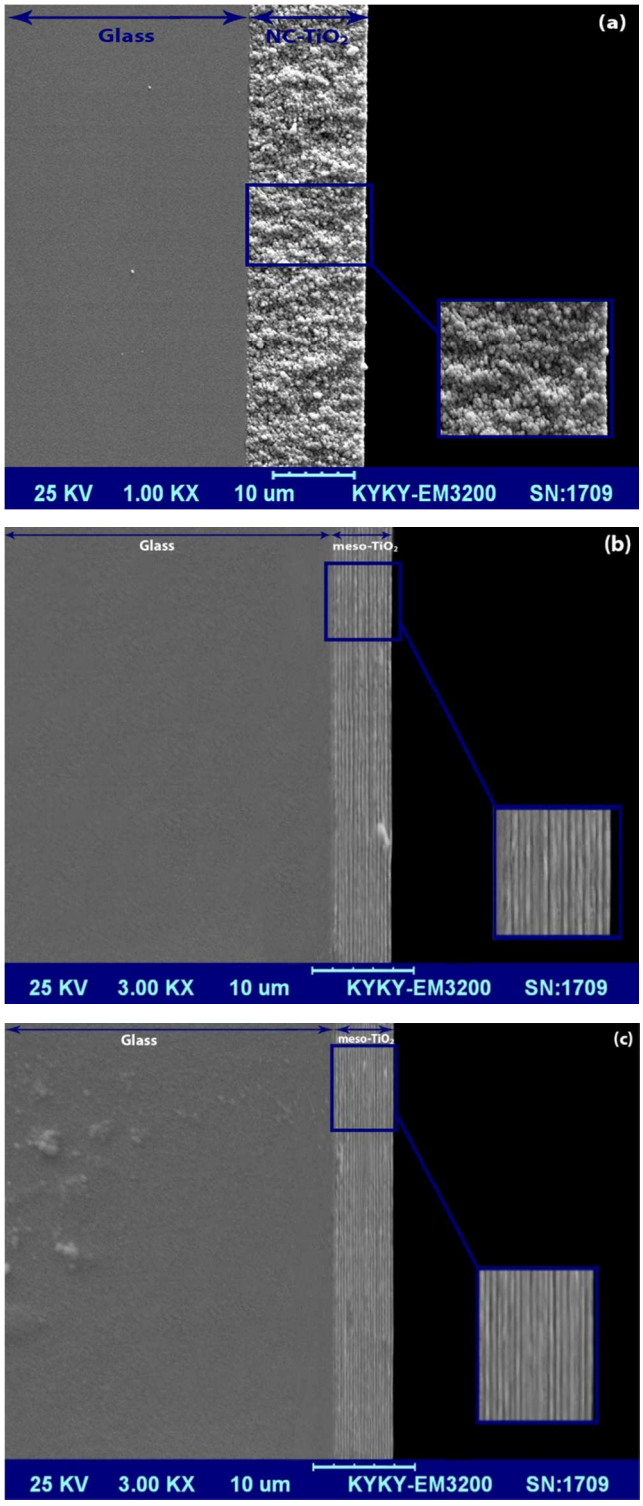

Figure 4. Cross sectional SEM images of: (a) 14µm NC-TiO_2 and mesoporous 5.7 µm thick titania films prepared by (b) dip and (c) spin coating methods.

Fig. 4 shows the cross-sectional SEM micrographs of the wormlike mesostructure films and the NC-TiO_2 film prepared by the Doctor-blading method commonly used in DSSCs. It is obvious that the layer by layer deposition leads to increase the thickness of the films. Fig. 4c shows that the preparation of a thick mesoporous films by spin coating method needs more

coating cycle than dip coating method with the same thickness (Fig. 4b). As shown in Fig. 4b and 4c, for preparation of a film with a thickness of about 5.7 µm, 15 and 20 layers require by dip and spin coating methods, respectively. These results confirm the values of the thickness obtained by ellipsometry.

The N_2 adsorption/desorption isotherms of wormlike titania films prepared by dip and spin coating methods are type IV with a H2 hysteresis loop (Fig. 5b and 5d). The H2 type hysteresis ascribes materials that are often disordered. Whereas N_2 adsorption/desorption isotherms of gridlike titania films prepared by dip and spin coating methods are type IV with a H1 hysteresis loop (Fig. 5a and 5c) because it displays parallel and nearly vertical branches between the adsorption and desorption isotherms. The H1 hysteresis typically represents the porous materials consisting of well-defined cylindrical-like pore geometry or agglomerates of approximately uniform spheres.[48] The BET specific surface areas for the wormlike mesoporous titania films obtained by dip and spin coating methods were calculated to be 139.62 and 132.86 m^2g^{-1}, respectively, with the pore volume of 0.235 and 0.231 cm^3g^{-1}, respectively. The BET surface areas for the gridlike mesoporous titania films prepared by dip and spin coating methods were also calculated to be 111.04 and 103.88 m^2g^{-1}, respectively, with the pore volume of 0.205 and 0.199 cm^3g^{-1}, respectively.

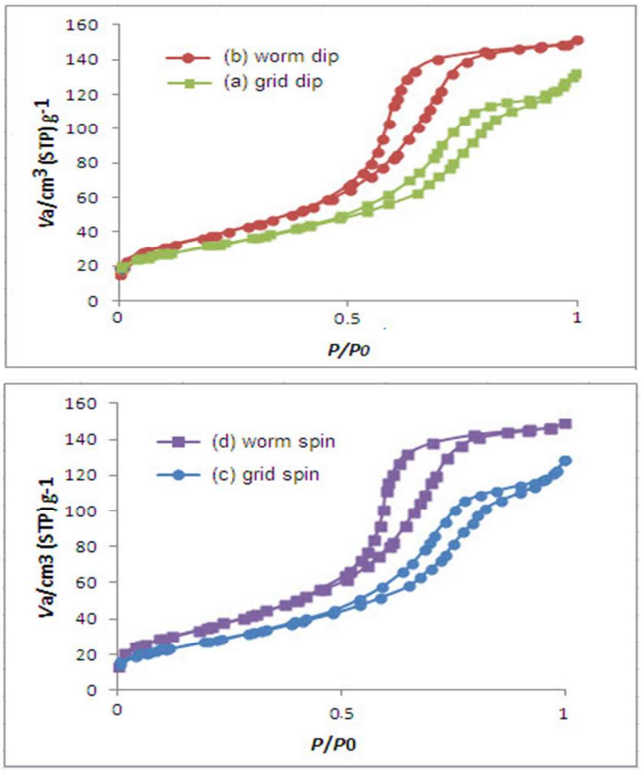

Figure 5. Nitrogen adsorption-desorption isotherm of: (a) grid like and (b) wormlike mesostructures related to 5.7 µm film prepared by dip coating methods, respectively, (c) and (d) N_2 adsorption-desorption spectra of the gridlike and wormlike mesostructures related to 5.7 µm film prepared spin coating techniques, respectively.

The efficiency of a sensitized TiO_2 photoanode is influenced by its surface area, expressed by the roughness factor, crystallinity, porosity and quality of crystal interconnects.[10, 32-34] The films bearing higher surface area adsorbs higher amounts of dye, and therefore, increases the light harvesting and cell performance. The maximization of the electrode surface area (roughness factor) is one of the obvious research targets in Grätzel cells. The roughness factor is defined as:

$$RF = \frac{A}{A_0} \quad (2)$$

Where A is the overall ''surface concentration'' of the dye (obtained by dye loading and expressed in moles per projected electrode area), and A_0 is the specific surface coverage (in moles per physical electrode area).[33,34] Zukalova *et al.*[33,34] and Dewalque *et. al*[10] calculated the roughness factors from this equation for 3 layers of titania mesoporous templated films with A_0= 0.31 molecules nm^{-2} for N719-dye.[33] For 1 µm (3 layers) thick P123 films, the experimental RFs are about 412 to 466,[33,34] and for 1 µm (3 layers) thick P123 wormlike films, the recalculated RF is about 640.[10] The recalculated RFs obtained from dye loading experiments performed on the films prepared in this study is reported in Table 2. The highest values presented in Table 2 are related to wormlike mesostructure films (3 layers) and among these, the wormlike titania film prepared by dip coating method has the highest dye loading value and RF. Moreover, the dye loading and roughness factor show similar orders (see eqn (2)).

Table 2. Dye loading and Roughness Factor values of 3-layer mesoporous titania templated films

Mesoporous Film	Dye loading/mol mm^{-2}	RF
Wormlike-dip coating	3.328×10^{-10}	646
Wormlike-spin coating	3.220×10^{-10}	625
Gridlike-dip coating	2.972×10^{-10}	577
Gridlike-spin coating	2.844×10^{-10}	552

In the next step, thicker mesoporous films were prepared through layer by layer deposition and their dye loading values were measured. The results are shown in Fig. 6. As can be seen, the thicker films have a more dye loading. However, this conclusion is valid only for the mesoporous films composed of 1-18 layers and 1-20 layers prepared by dip coating (Fig. 6a) and spin coating (Fig. 6b) methods, respectively, but for higher number of layers, this parameter reaches a saturation plateau. It can be related to the number of calcination steps. It seems that more than four calcinations steps caused a significant decrease in dye loading. This reduces the RF and therefore, reduces the dye loading. This is in agreement with the results reported previously.[32-34] The amount of ''amorphous'' TiO_2 in the mesoporous film can be minimized by thermal treatment. However, prolonged calcination also causes collapse of the mesopore morphology and the loss of active electrode area (roughness factor).[33] Obviously, the optimization of such mesoporous films for dye sensitized solar cells presents an interplay between the quality of anatase crystals and their surface area. Actually, to preparation of mesoporous films with a thickness of about 5.7µm, we need 15 layers with 3 calcination steps for dip coating and 20 layers with 4 calcination steps for spin coating method. Therefore, the roughness factor will increase certainly in these conditions.

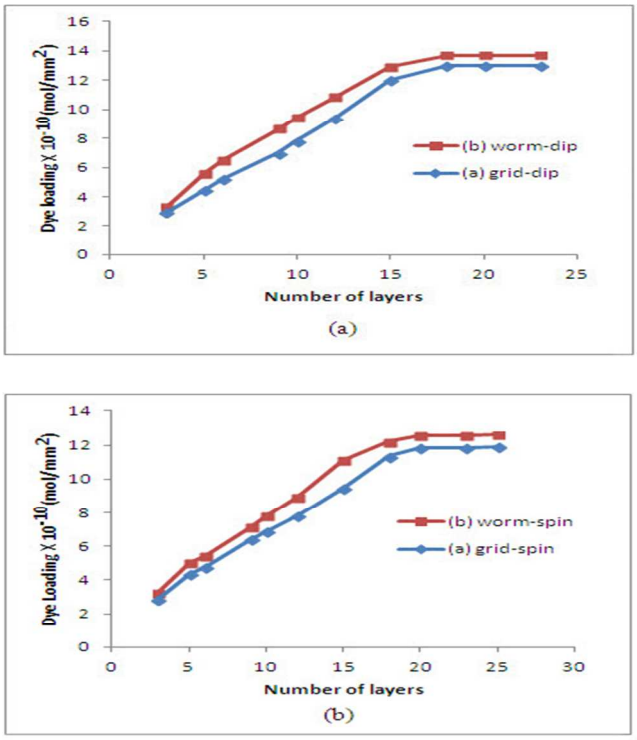

Figure 6. Dye loading expressed in moles of N719 dye per mm^2 of projected electrode area as a function of the number of layers for the films prepared by (a) dip and (b) spin coating.

Photovoltaic performances of mesoporous thick films

The wormlike and gridlike mesoporous thick films, prepared by dip and spin coating methods, bearing approximately similar thicknesses (5.7 µm) were used in DSSCs. Their photovoltaic data are reported in Table 3, and also the photocurrent density-voltage curves for fabricated DSSCs by these films are shown in Fig. 7. These data were compared with a 10 µm NC-TiO_2 film commonly used in DSSCs. From Table 3, it is evident that the crystallite size and RF values have a significant influence on the device performance. An increase is observed in the values of Jsc and Voc by increasing of RF and crystallinity. The Jsc parameter is highly dependent to the dye loading, and thus the surface area and pore connectivity. The prepared wormlike mesostructure films have the highest RF values, and therefore, the highest dye loading. As shown in the Table 3 and also Fig 7, the highest values of Jsc are observed for the wormlike films. On the other hand, the gridlike meso-films have the highest values of crystallinity, and therefore the highest Voc. As previously mentioned, the higher degree of crystallization has a positive effect on the Voc value; better electron injection and transport in the semiconductor phase as well as fewer recombination losses on grain boundaries.[10] Moreover, the values of Voc for all mesoporous photoanode cells are higher than NC-TiO_2 cells. This may be due to the position of the Fermi level of TiO_2 with respect to the redox potential of the electrolyte. With increasing the surface area in a mesoporous film, greater number of electrons would be generated due to the capture of more number of photons by dye molecules. By transferring of these electrons to the conduction band of the TiO_2 the electron density in the conduction band (CB) increases, which in turn shifts the Fermi level towards CB. In a DSSC, the Voc is essentially the difference between the Fermi level in TiO_2 under illumination and the redox potential of the electrolyte. Since the same electrolyte is used for all the cells, the increase in the voltage can be attributed to an increase in the density of electrons in the CB.[9] As shown in current-voltage curves of mesoporous templated cells in Fig. 7, the cell with higher photocurrent has lower Voc. This can be related to the fact that higher surface area electrodes often have lower Voc because the recombination rate is proportional to the surface area. Faster recombination means lower Voc. In other words, the open circuit photovoltage decreases because higher surface area means higher dark current.[39] Moreover, the crystallinity affects the Voc values. The higher degree of crystallization exerts a positive effect on the Voc value, due to better electron injection and transport in the semiconductor phase as well as fewer recombination losses on grain boundaries.[10] Moreover, anatas conductivity increases by enhancement in crystallinity of the mesoporous templated films which in turn increase the photovoltaic performance of the cells.[49] Meanwhile, Jsc of NC-TiO_2 cell is lower than that of meso-TiO_2. Lower Jsc for NC-TiO_2 photoelectrode based solar cells could be related to the fact that lower density of photoelectrons is generated due to its smaller roughness factor which reduces the amount of adsorbed dye (11×10^{-10} mol mm^{-2}). Clearly, the photovoltaic performance of our mesoporous titania films is the result of interplay between the roughness factor and crystallinity, while both parameters can be optimized by the number of layers and/or by heat treatment. This is also in accordance to the literature results.[32-34] The nanocrystalline titania device with a thickness of 10 µm provides 6.42% conversion efficiency while the lower thickness (5.7 µm) gridlike mesoporous photoanode prepared by spin coating provides 7.77% conversion efficiency. On the other hand, the gridlike meso films have a higher efficiency than wormlike meso films. It can be related to better crystallinity and pore connectivity and therefore improvement in electron transfer in the gridlike films. It seems that these parameters overcome the lower roughness in gridlike films. It should be noted that the preparation of the wormlike mesostructured films requires shorter time compared to gridlike films that are time consuming. In general, all prepared wormlike and gridlike mesoporous devices have conversion efficiencies higher than the NC-TiO_2 device. This is mainly related to the higher roughness and surface area in mesostructured films, along with pores connectivity, better dye loading and electrolyte impregnation. On the other hand, the improvement in Voc value due to the better crystallinity of the NC-TiO_2 film does not overcome the Jsc decrease due to its lower dye loading. As can be seen from Fig. 4a, the dye loading can increase up to 18 layers (about 6.8 µm) for mesoporous films in dip coating method. As far as we know, this thickness is the best thickness of mesoporous films for the DSSCs that reported up to now. Thus, two devices were built using the wormlike and gridlike films with this number of layers prepared by dip coating method. The results are shown in Table 4. As the film thickness increases, the photocurrent density (Jsc) and the solar cell efficiency (η) increase. It can be consistent with the fact that dye loading and RF increase up to 18 layers in dip coating method because of the improvement the films surface area up to 6.8 µm.

Table 3. Photovoltaic performances of the cells made by mesoporous 5.7 µm titania thick films and NC-TiO_2 with 10 µm thickness (RF values were recalculated from equation (2))

Device	Crystallite size/nm	Dye loading/ mol mm^{-2}	RF	IPCE(%) at 530 nm	V_{OC}/V	Jsc/mAcm^{-2}	FF	η (%)
Worm-dip	10.5	12.91×10^{-10}	2507	66.3	0.720	15.27	0.69	7.54
Worm-spin	11	12.58×10^{-10}	2443	65	0.729	14.93	0.68	7.35
Grid-dip	12.5	12.00×10^{-10}	2330	62	0.775	14.30	0.70	7.73
Grid-spin	14	11.81×10^{-10}	2293	60.8	0.780	14.01	0.71	7.77
NC-TiO_2	19	11.00×10^{-10}	2136	59.7	0.715	13.8	0.65	6.42

Highly efficient solar cells with efficiencies about 8.33% and 7.98% were obtained for gridlike and wormlike meso films prepared by dip coating without any doping or scattering layer. To the best of our knowledge, these values are the highest efficiencies that reported in the literatures for the mesoporous film devices. Unfortunately, our devices did not show more efficiency due to arising of plateau in dye loading and RF.

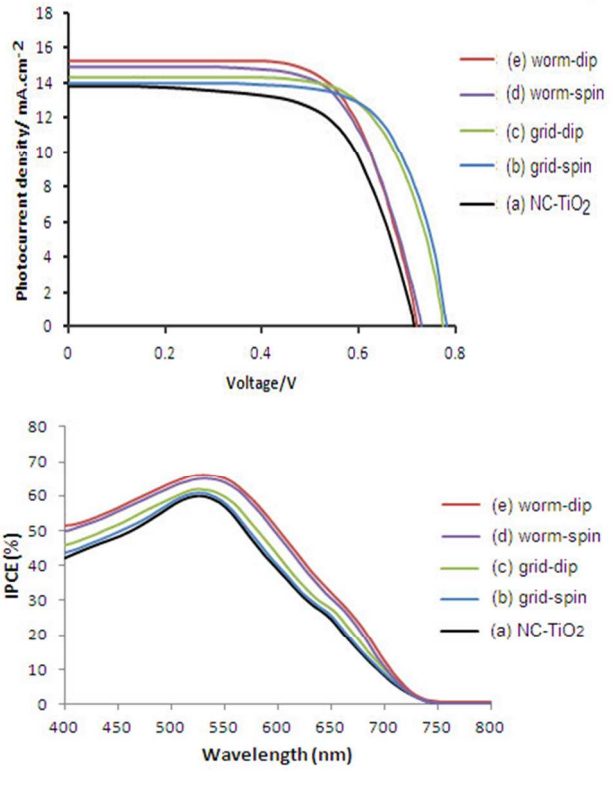

Figure 7. Current-voltage and IPCE curves of the DSSCs made of: (a) NC-TiO_2, and gridlike meso-film prepared by (b) spin and (c) dip coating methods. Current-voltage and IPCE curves of the DSSCs made of the wormlike meso-films prepared by (d) spin and (e) dip coating methods.

Fig. 7 also displays the IPCE of the solar cells made of the worm-like and the grid-like mesoporous titania films bearing 5.7 µm thickness. The cell made of the worm-like mesoporous titania film exhibited a higher quantum efficiency over the whole spectral range of 400-800 nm than that of its grid-like counterpart. The maximum IPCE of the mesoporous templated titania solar cells was 66.3% at 530 nm related to the worm-like mesoporouse titania photoanode obtained by dip coating method with highest surface area and dye loading. The maximum values of the IPCE spectra for other films at 530 nm are also listed in Table 3. It is clear that IPCE curves follow the loading of dye. In other words, the enhancement of IPCE reflects the increased dye uptake amount in the photoanode.

Table 4. Photovoltaic performances of the cells made by mesoporous 6.8 µm titania thick films (18 layers)

Device	Dye loading/ mol.mm^{-2}	Jsc/mA cm^{-2}	V_{OC}/V	FF	η (%)
Worm-dip	13.70×10^{-10}	16.07	0.725	0.69	7.98
Grid-dip	12.98×10^{-10}	15.33	0.778	0.70	8.33

There are various methods for synthesis of mesoporous films and many groups used these methods for preparation of mesoporous films and applied them in DSSCs. The solar cell efficiencies reported in the literature vary from each other due to different conditions and materials used in DSSC assembly such as dyes, electrolytes, surfactant etc. Thus, it is difficult to compare the efficiencies as an absolute criterion. However, our results were compared with some of the most important studies that used the EISA technique for synthesis of meso films and their application in DSSCs (Table 5). As can be seen, our mesoporous films have the highest thickness and solar cell efficiency compared to the other works owing to the optimal crystallinity and roughness factor in our synthesis protocol. The highest crystallite size is related to our mesostructure films which lead to improvement the Voc and Jsc, and therefore, solar conversion efficiency. Zukalova *et al*. reported a solar conversion efficiency of 5% for a 2.3 µm thick phosphor-doped templated-film.[34] However, chemical doping is not proper because it could modify the electronic structure of TiO_2 and induces electron–hole recombination. Furthermore, they used N945 dye which has a high molar extinction coefficient and a different electrolyte improving Voc. Zhang *et al*. prepared a 5-6µm thick meso film by spin coating method with a conversion efficiency of 6-7%.[37] But their solar cell efficiency is weakened when the film thickness was above 3.5 µm because of the serious cracks in the film. We did not observe any cracks in the films and also they required 60 layers to make a 5.08 µm film while in our synthetic protocol, 20 layers was sufficient for obtaining a 5.7 µm thickness by spin coating method. Dewalque *et al*. reported a solar conversion efficiency of 6.1% for a 4 µm (15 layers) wormlike thick templated-film obtained by dip coating method and sensitized with N719 dye.[10] Whereas we prepared a 5.7 µm thick film by deposition of 15 layers via dip coating technique and the solar conversion efficiency of about 7.54% was obtained. Sun *et al.* built a solar cell device with a bifunctional photoanode consisting of a 30-layer mesoporous TiO_2 film (4.15 µm) and a Degussa P25 TiO_2 light-scattering top-layer (4 µm), and obtained a 5.18% conversion efficiency.[21] However, all of the our mesoporous titania films show excellent photovoltaic performance compared to other literature without using any doping or scattering layer.

Table 5. Comparison of our results with some of the most important studies used the EISA technique for synthesis of meso-films and their application in DSSCs.[a]

Ref	Dye	Electrolyte composition	Crystallite size/nm	RF	Deposition technique	No. of layers	Thickness (μm)	η (%)
30	N945	0.6 M *N*-methyl-*N*-butylimidazolium iodide, 30 mM I_2, 0.5 M *tert*-butylpyridine, 0.1 M guanidine thiocyanate in acetonitrile/valeronitrile (85/15, v/v)	-	466	Dip coating	3	1	4.04
30	N719		-	466	Dip coating	3	1	2.95
33	N945	0.6 M *N*-methyl-*N*-butylimidazolium iodide, 40 mM I_2, 0.075 M lithium iodide, 0.26 M *tert*-butylpyridine, 0.05 M guanidine thiocyanate in acetonitrile/valeronitrile (85/15,v/v).	-	429	Dip Coating	5	1.3	4.52
34	N945		5-8	1300	Dip Coating	8	2.3	5.05
37[b]	N719	0.6 M 1-butyl-3-methylimidazolium iodide, 0.03M iodine, 0.1 M guanidine thiocyanate, and 0.5 M 4-*tert*-butylpyridine in acetonitrile/valeronitrile (85/15, v/v).	9.5-12	-	Spin coating	60	5-6 With large cracks in the film 2.5 Without crack	6-7 4.56
10	N719	Similar to ref. 37	-	1709	Dip Coating	15	4	6.1
21	N719	A commercial electrolyte (solaronix, Iodolyte AN-50)	3-5	-	Spin coating	30	4.15 with a P25 light-scattering top-layer (4 μm)	5.18
This study	N719	Presented in the text	10.5-14	2521	Dip Coating	18	6.8	8.33
This study	N719	Presented in the text	10.5-14	2293	spin Coating	20	5.7	7.77

[a]The used surfactant is P123.

[b]The used surfactant is F127.

Conclusions

Ordered and disordered mesoporous titania thick films up to about 7 μm in thickness were successfully synthesized by evaporation-induced self-assembly (EISA) process using dip and spin coating methods. To obtain crack-free thick films with high crystallinity and roughness factor, we used a stabilization step after each coating and a calcination step after each five layers. We also used the temperature of 20 ˚C for humidity ageing and deposition to avoid the formation of cracks. All of the mesoporous titania thick films showed excellent photovoltaic performance compared to other literature without using any doping or scattering layer. An 8.33% solar cell efficiency made of the ordered mesoporous films prepared by dip coating was achieved. As far as we know, this is the highest efficiency obtained by the photoanodes made of the mesoporous TiO_2 templated films.

Acknowledgements,

The financial support of this work by the University of Isfahan is acknowledged. Also, the authors greatly thank Prof. Thomas E. Mallouk and his collaborator, Dr Seung-Hyun Anna Lee, from the Pennsylvania State University, USA, for their useful scientific guidance and insightful comments. Authors also thank Prof. Michael D. McGehee from Stanford University, USA, Dr. Jennifer Dewalque, from university of liege, Belgium, and Dr. Mohsen Khosravi-Babadi from University of Isfahan for their invaluable scientific discussions.

Notes and references

Department of Chemistry, Catalysis Division, University of Isfahan, Isfahan 81746-73441, Iran. Fax: +98-31-36689732; Tel: +98-31-37932713; E-mails: mirkhani@sci.ui.ac.ir (Valiollah Mirkhani); moghadamm@sci.ui.ac.ir (Majid Moghadam).

1 J. Desilvestro, M. Grätzel, L. Kavan and J. Moser, *J. Am. Chem. Soc.*, 1985, **107**, 2988.
2 M. Grätzel, *Nature*, 2001, **414**, 338.
3 A. Yella, H. Lee, H. N. Tsao, C. Yi, A. K. Chandiran, M. K. Nazeeruddin, E.W. Diau, C.Y. Yeh, S. M. Zakeeruddin and M. Grätzel, *Scienc,* 2011, **334**, 629.
4 T. Hamann, R. Jensen, A. Martinson, H. Van Ryswyk and J. Hupp, *Energy Environ. Sci*., 2008, **1**, 66.
5 M. Grätzel, *Philos. Trans. R. Soc. A*, 2007, **365**, 993.
6 B. O'Regan and M. Grätzel, *Nature*, 1991, **353**, 737.
7 Y. Sakatani, D. Grosso, L. Nicole, C. Boissiere, G. J. A. A. Soler-Illia and C. Sanchez, *J. Mater. Chem*., 2006, **16**, 77.
8 C. Sanchez, C. Boissiere, D. Grosso, C. Laberty and L. Nicole, *Chem. Mater*., 2008, **20**, 682.
9 S. R. Gajjela, K. Ananthanarayanan, C. Yap, M. Grätzel and P. Balaya, *Energy Environ. Sci*., 2010, **3**, 838.
10 J. Dewalque, R. Cloots, F. Mathis, O. Dubreuil, N. Krins and C. Henrist, *J. Mater. Chem.,* 2011, **21**, 7356.
11 J. H. Pan, X. S. Zhao and W. I. Lee, *Chem. Eng. J*., 2011, **170**, 363.
12 S. H. Baeck, K. S. Choi, T. F. Jaramillo, G. D. Stucky and E.W. McFarland, *Adv. Mater*., 2003, 15, 1269.
13 K. S. Choi, H. C. Lichtenegger, G. D. Stucky and E. W. McFarland, *J. Am. Chem. Soc*., 2002, **124**, 12402.
14 H. M. Luo, L. Sun, Y. F. Lu and Y. S. Yan, *Langmuir,* 2004, **20**, 10218.
15 T. Xue, C. L. Xu, D. D. Zhao, X. H. Li and H. L. Li, *J. Power Sources,* 2007, **164**, 953.
16 C. J. Brinker, Y. Lu, A. Sellinger and H. Fan, *Adv. Mater*., 1999, **11**, 579.
17 C. J. Brinker, *Mater. Res. Bull.,* 2004, **29**, 631.

18 D. Grosso, F. Cagnol, G. J. A. A. Soler-Illia, E. L. Crepaldi, H. Amenitsch, A. Brunet-Bruneau, A. Bourgeois and C. Sanchez, *Adv. Funct. Mater.,* 2004, **14**, 309.
19 H. Yang, A. Kuperman, N. Coombs, S. Mamiche-Afara and G. A. Ozin, *Nature,* 1996, **379**, 703.
20 K. J. Edler, *Soft Matter,* 2006, **2**, 284.
21 Z. Sun, J. H. Kim, Y. Zhao, F. Bijarbooneh, V. Malgras and S. X. Dou, *J. Mater. Chem.*, 2012, **22**, 11711.
22 N. Nishiyama, S. Tanaka, Y. Egashira, Y. Oku and K. Ueyama, *Chem. Mater*. 2003, **15**, 1006.
23 S. Tanaka, N. Nishiyama, Y. Oku, Y. Egashira and K. Ueyama, *J. Am. Chem. Soc*., 2004, **126**, 4854.
24 K. J. Balkus, A. S. Scott, M. E. Gimon-Kinsel and J. H. Blanco, *Micropor. Mesopor. Mater.*, 2000, **38**, 97.
25 Y. Lu, R. Ganguli, C. A. Drewien, M. T. Anderson, C. J. Brinker, W.; Guo, Y. Gong, H. Soyez, B. Dunn, M. H. Huang and J. I. Zink, *Nature,* 1997, **389**, 364.
26 D. Grosso, *J. Mater. Chem*. 2011, **21**, 17033.
27 K. J. Edler and S. J. Roser, *Int. Rev. Phys. Chem*., 2001, **20**, 387.
28 S. Sokolov, B. Paul, E. Ortel, A. Fischer and R. Kraehnert, *Langmuir*, 2011, **27**, 1972.
29 C. Boissiere, D. Grosso, A. Chaumonnot, L. Nicole and C. Sanchez, *Adv. Mater*. 2011, **23**, 599.
30 M. Zukalova, A. Zukal, L. Kavan, M. K. Nazeeruddin, P. Liska and M. Grätzel, *Nano Lett*., 2005, **5**, 1789.
31 K. Hou, B. Tian, F. Li, Z. Bian, D. Zhao and C. huang, *J. Mater. Chem.*, 2005, **15**, 2414.
32 J. Prochazka, L. Kavan, V. Shklover, M. Zukalova, O. Frank, M. Kalbac, A. Zukal, H. Pelouchova, P. Janda, K. Mocek, M. Klementova and D. Carbone, *Chem. Mater*., 2008, **20**, 2985.
33 M. Zukalova, J. Prochazka, A. Zukal, J. H. Yum and L. Kavan, *Inorg. Chim. Acta*, 2008, **361**, 656.
34 M. Zukalova, J. Prochazka, A. Zukal, J. H. Yum, L. Kavan and M. Grätzel, *J. Electrochem. Soc*., 2010, **157**, H99.
35 P. C. Angelome, L. Andrini, M. E. Calvo, F. G. Requejo, S. A. Bilmesand and G. J. A. A. Soler-Illia, *J. Phys. Chem. C*., 2007, **111**, 10886.
36 H. J. Nam, T. Amemiya, M. Murabayashi, K Itoh, *J. Phys. Chem. B*, 2004, **108**, 8254.
37 Y. Zhang, Z. B. Xie and J. Wang, *ACS Appl. Mater. Interfaces,* 2009, **1**, 2789.
38 M. J. Cass, A. B. Walker, D. Martinez and L. M. Peter, *J. Phys. Chem. B,* 2005, **109**, 5100.
39 S. H. A. Lee, N. M. Abrams, P. G. Hoertz, G. D. Barber, L. I. Halaoui and T. E. Mallouk, *J. Phys. Chem. B,* 2008, **112**, 14415.
40 M.R. Baklanov and K.P. Mogilnikov, *Microelectron. Eng.,* 2002, **64**, 335.
41 E. L. Crepaldi, G. J. A. A. Soler-Illia, D. Grosso, F. Cagnol, F. Ribot and C. Sanchez, *J. Am. Chem. Soc*., 2003, **125**, 9770.
42 G. J. A. A. Soler-illia, C. Sanchez, B. Lebeau and J. Patarin, *Chem. Rev*., 2002, **102**, 4093.
43 J. H. Pan and W. I. Lee, *New J. Chem.,* 2005, **29**, 841.
44 H. Uchida, M. N. Patel, R. A. May, G. Gupta, K. J. Stevenson and K. P. Johnston, *Thin Solid Films,* 2010, **518**, 3169.
45 K. M. Coakley and M. D. McGeheea, *Appl. Phys. Lett.,* 2003*,* **83***,* 3380.
46 R. Zhou, Q. Zhang, E. Uchaker, J. Lan, M. Yin and G. Cao, *J. Mater. Chem. A*, 2014, **2**, 2517.
47 W. Li, Z. Wu, J. Wang, A. A. Elzatahry and D. Zhao, *Chem. Mater*., 2014, **26**, 287.
48 Z. A. ALOthman, *Materials,* 2012, **5**, 2874.
49 S. Guldin, S. Hüttner, P. Tiwana, M. C. Orilall, B. Ülgüt, M. Stefik, P. Docampo, M. Kolle, G. Divitini, C. Ducati, S. A. T. Redfern, H. J. Snaith, U. Wiesner, D. Eder and U. Steiner, *Energy Environ. Sci.* 2011, **4,** 225.

Highly efficient DSSCs were achieved by Worm-like and grid-like mesoporous thick templated photoanodes prepared by spin and dip coating methods.